

NASA-CR-204710

Reprinted from the preprint volume of the 9th Conference on Atmospheric Radiation, 2-7 February 1997, Long Beach, California, by the AMS, Boston, Massachusetts

P1.18 SATELLITE ESTIMATES OF THE DIRECT RADIATIVE FORCING OF BIOMASS BURNING AEROSOLS OVER SOUTH AMERICA AND AFRICA

Sundar A. Christopher¹, Min Wang¹, Donna V. Kliche¹, Todd Berendes¹, Ronald M. Welch¹ and S.K. Yang²¹Institute of Atmospheric Sciences, South Dakota School of Mines and Technology, Rapid City, SD²Climate Prediction Center/NCEP, Washington, DC

1. INTRODUCTION

Atmospheric aerosol particles, both natural and anthropogenic are important to the earth's radiative balance. They scatter the incoming solar radiation and modify the shortwave reflective properties of clouds by acting as cloud condensation nuclei (CCN). The first effect is termed as "direct radiative forcing" and the second, "indirect radiative forcing". Although it has been recognized that aerosols exert a net cooling influence on the atmosphere (Penner *et al.*, 1994; Charlson *et al.*, 1992), this effect has received much less attention than the radiative forcings due to greenhouse gases and clouds. The radiative forcing due to aerosols is comparable in magnitude to current anthropogenic greenhouse gas forcing but opposite in sign (Houghton *et al.*, 1992). One contributing factor for the inability of the current climate models to accurately estimate surface temperatures may be due to the inaccurate characterization of aerosol effects. Therefore it is important to provide adequate validation information on the spatial, temporal and radiative properties of aerosols. This will enable us to predict realistic global estimates of aerosol radiative effects more confidently.

Biomass burning, which is widely prevalent in the tropics (Crutzen and Andreae 1990) is due to savanna fires, shifting cultivation practices, deforestation, fuel wood use, and burning agricultural residues (Hao and Liu 1994). Although biomass burning activities are intense in the dry season, which is between December and March in the Northern hemisphere, and between June and September in the Southern Hemisphere, burning can take place whenever there is plant material dry enough to burn (Andreae, 1991). In South America, forest fires dominate the selva region, while agricultural burning due to savanna fires dominate the cerrado region. In tropical Africa, more than two thirds of the biomass burned is due to savanna fires, while the remaining portion is due to forest fires. In tropical Asia, shifting cultivation, fuel wood use, and deforestation provide for the majority of the burning with less than 10% of the burning in the savannas. Due to these activities, there is widespread

concern about the loss of biodiversity, spread of human and plant diseases via colonization, increase in concentrations of greenhouse gases, changes on the earth's radiative energy budget, effects on atmospheric chemistry and increases in surface albedo and water runoff. The implications of these activities on both regional and global scales are relatively unknown.

Current studies utilize some form of the radiative transfer equation to estimate the direct and indirect radiative forcing of biomass burning aerosols (Anderson *et al.*, 1996; Penner *et al.*, 1994). Using various available information of biomass burning aerosols, Penner *et al.* (1994) estimate that the global radiative forcing of smoke for both the direct and indirect effect is on the order of about -2W/m^2 which is comparable to the cooling by the sulfate aerosols (Charlson *et al.*, 1992). Using more recent values on biomass burning, Anderson *et al.* (1996) estimate that the average biomass burning plume reduces surface radiation by about $10\text{-}25\text{ W/m}^2$ over land and sea. Several assumptions have to be made in order to estimate radiative forcing values from radiative transfer equations. For example, the following variables must be known: (1) rate of biomass burning, (2) fraction of burnt material that goes into smoke, (3) lifetime of smoke in the atmosphere, (4) surface albedo, (5) fraction of clouds, (6) optical properties of aerosols (optical depth, particle size), (7) atmospheric conditions that influence aerosol properties, and (8) aerosol mass absorption and scattering efficiency. These estimates are drawn from limited samples during field experiments and laboratory research. Another approach is to obtain the direct radiative forcing values from satellite data (Christopher *et al.*, 1996). In this technique, the smoke from biomass burning is first identified using satellite imagery such as the Advanced Very High Resolution Radiometer (AVHRR) Local Area Coverage (LAC) data. Then using collocated broadband measurements from the Earth Radiation Budget Experiment (ERBE), the direct radiative forcing of the smoke from biomass burning can be estimated. Using eleven images over South America, previous work showed the net radiative forcing of smoke from biomass burning aerosols over South America is about -36 W/m^2 . The current study utilizes 66 AVHRR LAC images and coincident ERBE data to characterize the fires, smoke and radiative forcings of biomass burning aerosols over four major ecosystems within South America.

Corresponding author address: Sundar A. Christopher, Institute of Atmospheric Sciences, South Dakota School of Mines and Technology, 501 E. St. Joseph Street, Rapid City, SD 57701-3995.

2. DATA SETS AND AREA OF STUDY

The Earth Radiation Budget Experiment launched in 1984 by NASA, used broadband measurements in the shortwave (0.25-4 μm), longwave (4-50 μm) and total (0.25-50 μm) part of the electromagnetic spectrum from three satellites (NOAA-9, NOAA-10, and ERBS) to understand the radiation balance of the earth-atmosphere system. Each satellite was equipped with a scanner and a non-scanner to estimate the top of atmosphere fluxes. The present study utilizes the scanner measurements from the NOAA-9 satellite. Considering the point spread function, the nominal spatial resolution of the ERBE scanner is about 35 km. Although the AVHRR data are available from February 1985-January 1988, the ERBE scanner onboard NOAA-9 failed in January 1987. Therefore, only two biomass burning seasons can be analyzed.

The AVHRR data that is used in this study, is of the LAC form with an instantaneous field of view at the satellite subpoint of about 1.1 km while at the edge of the scan it degrades to about 4-4.5 km in the cross-track direction and 1.5-2 km in the along-track direction. The AVHRR views the earth through a cross track angle of about $\pm 55.4^\circ$ from nadir and measures radiation in five channels (0.58-0.68 μm ; 0.7-1.1 μm , 3.5-3.9 μm , 10.5-11.5 μm , and 11.5-12.5 μm). Channels 4 and 5 have onboard calibration whereas channels 1, 2, and 3 have no onboard calibration. For NOAA-9, the north-bound equator crossing is at 1420 Local Solar Time (LST), and it is during this time that AVHRR LAC is traditionally available. Since the spatial resolution of the AVHRR and ERBE data are different, the data are first collocated by finding the closest latitude and longitude of an AVHRR pixel corresponding to the ERBE pixel. Once the closest center pixel is determined, an average of 37X37 pixels is assumed to correspond to the footprint of the ERBE pixel. Collocation accuracies are checked by comparing the AVHRR channel 1 reflectances and the channel 4 temperatures of the 37X37 pixel box with the ERBE shortwave and longwave flux values respectively. Linear correlation coefficients are usually greater than 90%. The remaining 10% probably accounts for the different spectral band-passes of the two instruments.

In the present study, sixty-six images from July (6 images), August (23 images), September (22 images), and October (15 images) are used to characterize the fires, smoke and the radiative forcing as a function of ecosystems. However, only the August 1985 results are discussed. According to the Olson world ecosystem data base (Olson, 1991), there are four major ecosystems within South America. The four ecosystems are 1) Tropical Rain Forest (TRF), 2) Tropical Broadleaf Seasonal (TBS), 3) Savanna/Grass/Seasonal Woods (SGW), and 4) Mild-

Warm/Hot/Grass/Shrub (MGS). Figure 1a shows these four ecosystems over South America.

3. METHODOLOGY

The preprocessed AVHRR images are first classified into clear and cloudy regions using a new technique called the paired-histogram approach (Berendes *et al.*, 1996) that is being developed as part of the Clouds and the Earth's Radiant Energy (CERES) global cloud masking program. Region labeling of fifteen classes (water, land, smoke, sunglint, land etc.) is performed manually and a total of 185 features (the five calibrated AVHRR pixel values, channel differences, ratios, etc.) are calculated to develop an algorithm that separates the various classes.

After the images are separated into one of fifteen classes, the next step is to detect pixels with fires for clear sky regions. There is a large body of literature for fire detection schemes (for a review see Kaufman and Justice 1994). Most of these methods use some kind of a threshold to eliminate clouds. The paired-histogram classifier offers a definite advantage by eliminating clouds, sun-glint and water so further processing of fire pixels over land can be performed. In the present study, fire detection is performed using a modified version of the Goddard algorithm (Kaufman and Justice 1994). For cloud free pixels within a scan angle of $\pm 45^\circ$, a series of spectral and spatial tests are performed to determine if a clear pixel has fire or no fire. Selected images are then used to visually determine if fires were accompanied by smoke plumes.

One of the classes that is identified by the paired-histogram classifier is smoke. Approximately 38,888 smoke samples were manually selected that were used as input to the algorithm. Preliminary results from 18 images over South America show that smoke pixels are classified with a 95% accuracy. The remaining 5% of the smoke pixels were classified as land. A number of selected images were also used to visually inspect the accuracy of the smoke detection algorithm. Once the smoke and clear sky pixels are identified, the collocated ERBE pixel is used to determine the TOA shortwave and longwave fluxes for smoke and clear sky. Clear sky statistics are accumulated for by ensuring that the entire grid box was classified as clear land by the algorithm. However, it is often difficult to obtain smoke samples that completely cover an ERBE footprint. Therefore an ERBE pixel was classified as "smoky" if at least 50% of the AVHRR pixels within an ERBE footprint was covered with smoke.

4. RESULTS

In this paper only the August 1985 results for South America are discussed. Figure 1b shows a 0.5°X0.5° gridded map with pixels identified as fire.

The number of fires were accumulated for each day for that entire month. Twenty-three images were used to produce this figure. The fires are centered around Rondonia, and Matto Grosso, in agreement with previous studies (Tucker *et al.*, 1984). Maximum number of fire counts is about 500, shown by darker shades of grey. Figure 1c shows the frequency distribution of fires for the four major ecosystems. During August 1985, fires were predominantly in the tropical broadleaf, savanna, and grass shrub ecosystems, with 38% of fires occurring in the savanna. Less than 1% of the fires were found in the tropical rainforest region for this month, which made the statistics unreliable for computing the aerosol radiative forcing.

In order to compute the instantaneous aerosol radiative forcing, the following terms are defined: 1) SWARF = $S_0 (\alpha_{clr} - \alpha_{aer})$, and 2) LWARF = $(LW_{clr} - LW_{aer})$, where SWARF is the shortwave aerosol forcing in W/m^2 ; LWARF is the longwave aerosol radiative forcing in W/m^2 ; α is broadband albedo; LW is the longwave flux in W/m^2 ; and the subscripts *clr* and *aer* stand for clear and aerosol sky regions respectively. The net radiative forcing (NETARF) is obtained by adding the shortwave and longwave radiative forcing terms. Note that the values defined in this way are instantaneous and contain no spatial or temporal averaging.

Figure 1d shows the radiative forcing estimates from August 1985. As mentioned before, the tropical rain forest category did not have adequate samples to compute the radiative forcing terms. For all three ecosystems, the instantaneous shortwave radiative forcing values are negative, which shows the reflective nature of the smoke. Maximum SWARF values of $-51.5 W/m^2$ are found for the grassland ecosystem. The LWARF values are positive which shows that the effective radiating temperature for the smoke is lower than that of land. Maximum values are $17.9 W/m^2$ are found for the grassland ecosystem. Therefore, the net radiative forcing values are negative which implies a net "cooling" effect. The maximum net radiative forcing values are for the TBS ecosystem. The instantaneous NETARF values range from -33.6 to $-42.8 W/m^2$ which are consistent with previous estimates (Christopher *et al.*, 1996). There appears to be only a $9 W/m^2$ change in the net radiative forcing values as a function of ecosystem.

Acknowledgments. This research was sponsored by NASA grant NAGW-3740, managed by Dr. Robert J. Curran and the NASA Young Investigator Program, managed by Dr. Ghassem Asrar. Special thanks are extended to Kwo-Sen Kuo, Joyce Chou, Min Wang, and Donna Kliche for their programming help. The ERBE data were obtained through the Langley DAAC.

References

- Anderson, B. E., W. B. Grant, G. L. Gregory, E. V. Browell, J. E. Collins, Jr., G. W., Sachse, D. R. Bagwell, C. H. Hudgins, D. R. Blake, and N. J. Blake, 1995: Aerosols from Biomass Burning over the Southern Tropical Atlantic Region: Distributions and Impact. *J. Geophys. Res.*, special issue TRACE-A.
- Andreae, M. O., 1991: Biomass burning: Its history, use, and distribution and its impact on environmental quality and climate. In *Global Biomass Burning*, Edited by J. S. Levine, 1-21.
- Berendes, T. A., A. Pretre, R. C. Weger, D. V. Kliche, and R. M. Welch, 1996: A paired-histogram rule-base approach for cloud and smoke classification applied to polar and desert regions and South America. *submitted to JGR-Atmos.*
- Charlson, R. J., S. E. Schwartz, J. M. Hales, R. D. Cess, J. A. Coakley Jr., J. E. Hansen, and D. J. Hofmann, 1992: Climate forcing by anthropogenic aerosols. *Science*, **255**, 423-430.
- Christopher, S. A., D. V. Kliche, J. Chou, and R. M. Welch, 1996b: First estimates of the radiative forcing of aerosols generated from biomass burning using satellite data. Accepted for publication in *J. Geophys. Res.*
- Crutzen, P. J., and M. O. Andreae, 1990: Biomass burning in the tropics: Impact of atmospheric chemistry and biogeochemical cycles. *Science*, **250**, 1669-1678.
- Hao, W. M., and M-H. Liu, 1994: Spatial and temporal distribution of biomass burning. *Global Biogeochemical Cycles*, **8**(4), 495-503.
- Houghton, J. T., G. J. Jenkins, and J. J. Ephraums, eds, 1990: *Climate change: The IPCC Scientific Assessment* (Report prepared for the Intergovernmental Panel on Global Climate Change). Cambridge University Press, Cambridge, 362pp.
- Kaufman, Y., and C. Justice, 1994: Fire Products. *The MODIS Algorithm Theoretical Basis Document*, Version 1.2.2 (Feb. 21, 1994; EOS ID# 2741), 48pp.
- Olson, J. S., 1991: World Ecosystems (WE1.3 and WE 1.4) Digital Raster data on global Geographic (LAT/lon) 180X360 and 1080X2160 grids. Available from NOAA National Geophysical Data Center. Boulder, Colorado.
- Penner, J. E., R. J. Charlson, J. M. Hales, N. S. Laulainen, R. Leifer, T. Novakov, J. Ogren, L. F. Radke, S.E. Schwartz, and L. Travis, 1994: Quantifying and minimizing uncertainty of climate forcing.
- Tucker, C. J., N. N. Holben, and T. E. Goff, 1984: Intensive Forest Clearing in Rondonia, Brazil, as Detected by Satellite Remote Sensing. *Rem. Sens. Environ.*, **15**, 255-261.

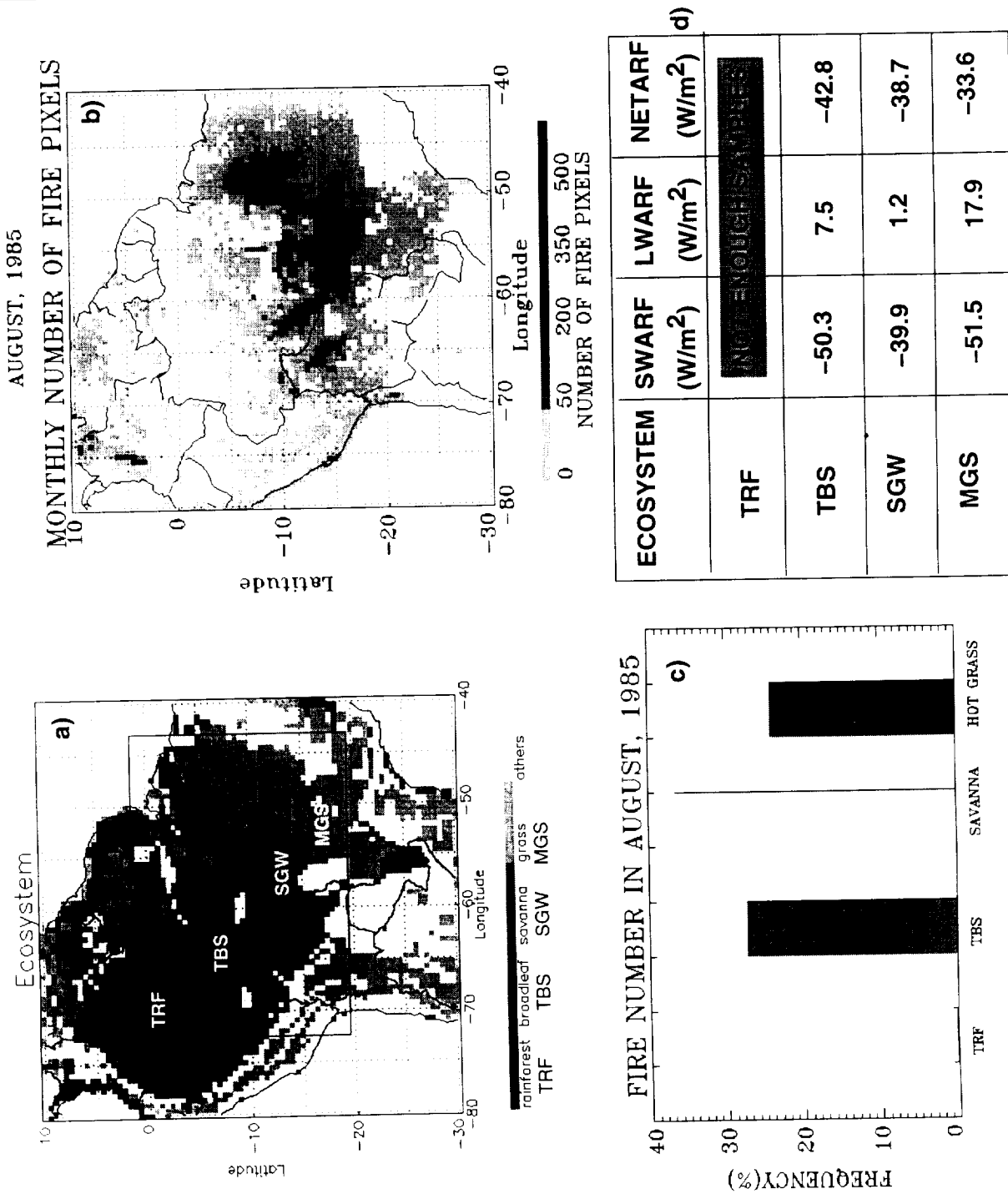


Figure 1 : Biomass burning results for August 1985. a) Major ecosystems within South America. b) Spatial distribution of fires c) Frequency of fires for four major ecosystems and d) Radiative forcing estimates from ERBE data.